DOI 10.5162/Ultrasonic2025/D3-a6

Exploring Laser-Induced Ultrasound for Fruit Quality: Multi-Fruit Validation and Avocado Ripening Studies

J. L. Castaño[1] and J. L. Ealo[2]
[1]Universidad del Valle, Mechanical Engineering School, Cali, Colombia
[2]Universidad del Valle, Centre for Bioinformatics and Photonics (CIBioFi), Cali, Colombia
jose.luis.castano@correounivalle.edu.co

Abstract: We evaluate a laser-generated ultrasound method for non-destructive fruit assessment. Unlike prior full-contour studies, this paper provides a non-destructive method for determining phase velocity and attenuation over a short linear segment of the surface. Trials on kiwi, banana, and avocado revealed strong attenuation sensitivity to viscoelastic differences. In avocados, postharvest monitoring showed measurable attenuation drops with ripening, while phase velocity remained stable. The method detected structural changes before visible softening and may support early pest damage detection and automated quality grading.

Keywords: Fruit, Laser ultrasonics, attenuation, phase velocity, Non destructive monitoring

Introduction

Non-invasive techniques have emerged as effective alternatives for characterizing internal properties of fruits without compromising their integrity. Among these, optical methods such as hyperspectral imaging and near-infrared spectroscopy (NIR) have gained prominence due to their capacity to detect internal bruises and monitor chemical composition. However, these optical methods face limitations when applied to thick-skinned fruits due to reduced light penetration and sensitivity to surface heterogeneity. These constraints hinder their effectiveness in assessing mechanical properties during postharvest changes such as ripening.

Laser-induced ultrasound (LIUS) offers a compelling solution by combining deep tissue penetration with high spatial and temporal resolution [1]. This approach enables the remote generation and detection of elastic waves, allowing the measurement of mechanical parameters, such as wave attenuation and velocity, in fruits that evolve during ripening. Measurements have shown a close relationship with structural changes in apples [2, 3], kiwifruit [4], and mangoes [5] during post-harvest periods. While LIUS offers promising capabilities, its application in tropical and structurally complex fruits remains underexplored.

This study proposes and validates a non-contact optoacoustic method to characterize the elastic behavior of fruit tissues, focusing on a spatial profile of 10 mm linear scan. A pulsed laser generates surface-guided waves on the fruit exocarp, while a laser Doppler vibrometer captures the dynamic response. Initial experiments on bananas (*Musa acuminata*), kiwis (*Actinidia deliciosa*), and avocados (*Persea americana*, cv. Fuerte) demonstrated the feasibility of generating and processing spatiotemporal wavefields. Avocados were further selected for postharvest ripening analysis.

The mechanical evolution of avocado tissue was evaluated by extracting attenuation coefficients and phase velocity dispersion curves across multiple days. Signals were processed using dynamic time warping (DTW) in the time domain and slant-stacking in the frequency domain, enabling a comparative analysis throughout ripening stages.

The experimental configuration and signal processing methods are described, followed by results on attenuation and phase velocity in the three fruits. The study examines their evolution during avocado ripening and summarizes the main conclusions and future perspectives.

Methodology

Fig. 1 illustrates the optoacoustic implementation used. A Nd:YAG laser (532 nm, <10 ns, 20 Hz, 2 mJ, 1 mm spot) generated elastic waves on the exocarp of the fruits. The laser energy was adjusted to maintain operation within the thermoelastic regime, avoiding tissue damage. The mechanical response was captured by a laser Doppler vibrometer (LDV) (Polytec OFV-505, 10 mm/s/V sensitivity, up to 250 kHz bandwidth). Beam delivery used collimating optics and galvanometric scanning for linear surface profiling under non-contact excitation. Signals were acquired with an oscilloscope (Rigol DS6104) and transferred to a computer for digital processing. To improve the signal-to-noise ratio, a thin layer of white ink was applied to the linear profile.

Riped kiwi (*Actinidia deliciosa*), banana (*Musa acuminata* cv. Cavendish), and avocado (*Persea americana*, cv. Fuerte) were tested under 20 ± 1 C and

DOI 10.5162/Ultrasonic2025/D3-a6

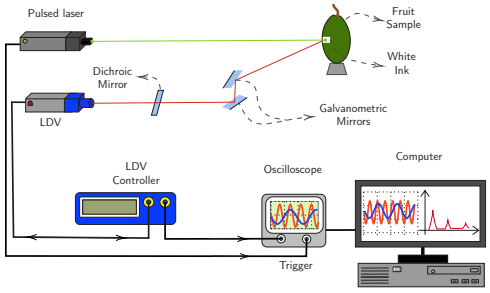

Fig. 1: Experimental scheme for laser-induced ultrasound mapping over a short linear segment of fruit surface.

$70\pm5\%$ RH. Avocado was monitored daily over 7 days of ripening. The LDV scanning range was $[-5, +5]$ mm and a distance interval of 0.2 mm for banana. The range for avocado and kiwi was $[-10, +10]$ mm with 0.1 mm intervals. All waveforms were zero-padded and low-pass filtered (250 kHz cutoff).

After preprocessing, attenuation and phase velocity estimations were performed. Wave attenuation was assessed with an exponential model $A(x) = A_0 e^{-\mu x}$, where A_0 is the amplitude at $x = 0$, $A(x)$ at position x, and μ the linear attenuation coefficient. The μ values were selected based on the fit yielding the highest coefficient of determination (R^2). Attenuation in dB/mm was obtained via $\alpha = 8.686 \cdot \mu$.

Main phase-front velocities in the time domain were estimated using the Dynamic Time Warping (DTW) algorithm [6, 7, 8]. The reference was typically the closest trace to the laser impact; if inadequate, a nearby high-quality trace within $\pm$0.4 mm was used. Time-of-flight Δt was extracted, and velocity was estimated via linear fits of the predominant wave phase front.

To extract dispersion curves, slant-stacking and phase-shift methods were applied [9, 10, 11, 12, 13]. Each signal was Fourier transformed, normalized, and phase-corrected using trial velocities. The corrected spectra were coherently summed to form a spectral coherence matrix S(f,c), from which the dominant phase velocities were identified. Amplitude maxima in S(f,c) were semi-automatically selected by visual inspection and localized peak detection across frequency bands.

Results and discussion

In order to compare the responses between fruits, Fig. 2 shows attenuation (α) for kiwi, avocado, and banana.

Within 25–100 kHz, kiwi exhibits the highest attenuation, avocado intermediate, and banana the lowest. Kiwi rises from 0.22 dB/mm to 1.0 dB/mm; avocado from 0.18 to 0.75 dB/mm; and banana from 0.14 to

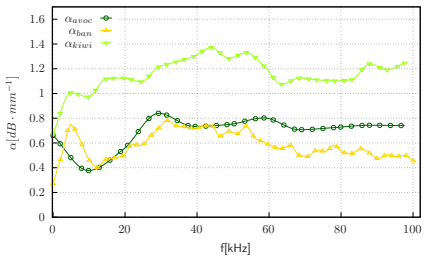

(a) α vs f

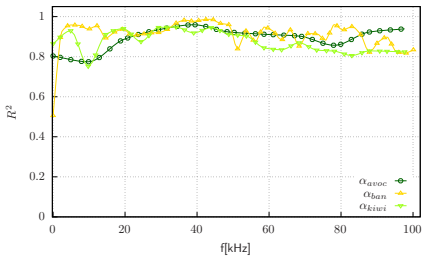

(b) R^2 vs f

Fig. 2: (a) Attenuation coefficient (α) for kiwi (light-green), avocado (dark-green), and banana (yellow) as a function of frequency, obtained from exponential fits of the amplitude-decay model. (b) Goodness–of-fit (R^2) for attenuation linear fits, which confirmed the reliability of the extracted α values in the 0–100 kHz band.

0.60 dB/mm. This reflects the higher viscoelasticity and reduced exocarp thickness of kiwi. Kiwi's steeper curve slope indicates stronger frequency-dependent dissipation, consistent with its high water content. All fits showed R^2>0.8, confirming model reliability (Fig. 2b). Differences in attenuation reflect variations in tissue stiffness, layered structure and moisture content among fruits.

Fig. 3 shows space-time wavefields for each fruit. Orange $\times$ markers indicate DTW-aligned time-of-flights; red lines show linear fits. The estimated velocities were 48.96 $\pm$ 2.7 m/s (banana), 82.29 $\pm$ 7.59 m/s (kiwi), and 78.41 $\pm$ 14.95 m/s (avocado) in each predominant wave phase front. These values reflect the stiffness and hydration levels of each fruit: kiwi exhibited the fastest propagation due to its compliant and water-rich structure, followed by avocado with a stiff exocarp, while banana, with its thicker and high fiber-content, supported the slowest surface wave speed.

Dispersion curves in Fig. 4 confirm the velocity trends observed in time-domain wavefields. Banana exhibits the lowest phase velocities, ranging from 46.8 to 68.7 m/s, limited above 75 kHz due to signal attenuation. Kiwi shows higher velocities ranging from 89.7 to 130.4 m/s, with avocado presenting intermediate

DOI 10.5162/Ultrasonic2025/D3-a6

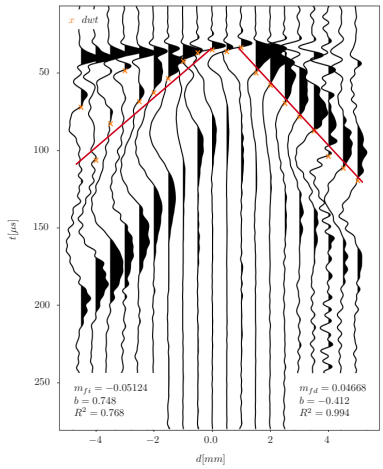

(a) Wavefield banana

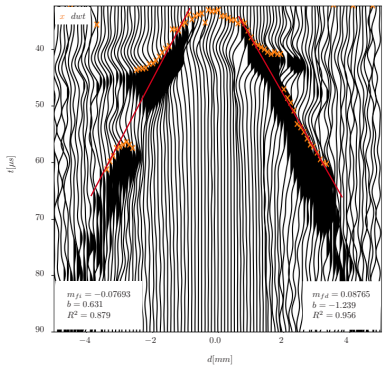

(b) Wavefield kiwi

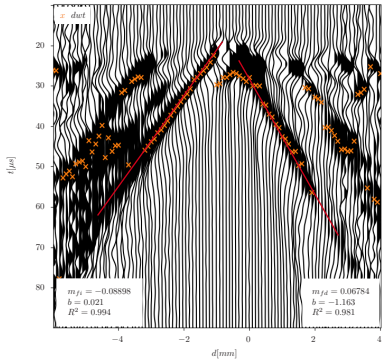

(c) Wavefield avocado

Fig. 3: Time-domain wavefields along the laser-scan line for (a) banana, (b) kiwi, and (c) avocado. Black traces plot the out-of-plane surface velocity; orange $\times$ marks show the DTW-derived time-of-flight Δt for each trace. Red lines represent linear fits whose slopes (m_{fd}, m_{fi} in mm/μs) appear at the lower corners of every plot.

values. The relative increases in phase velocity across the frequency range were 71% (kiwi), 78% (avocado), and 47% (banana). These results indicate that the

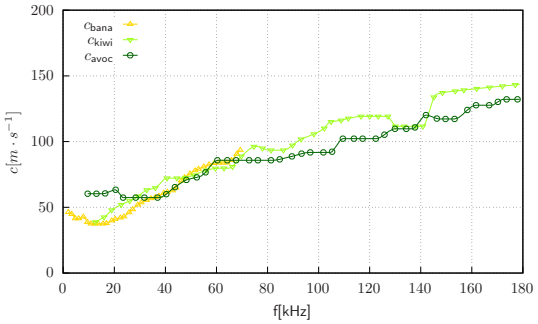

Fig. 4: Dispersion curves for banana, kiwi, and avocado: phase velocity as a function of frequency.

LIUS technique is sensitive to variations in fiber composition, moisture content, and structural differences at the exocarp–mesocarp interface.

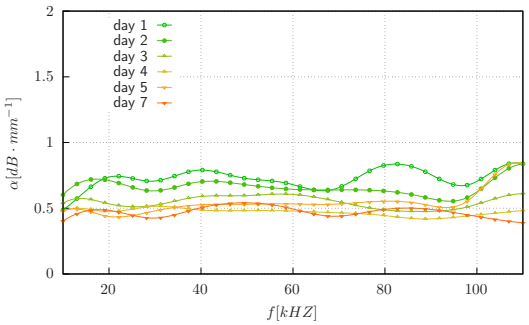

Fig. 5: Attenuation curves (α) of avocado tissue measured from day 0 to day 7 of postharvest ripening. Each curve corresponds to a distinct stage in the maturation process. All exponential fits showed correlation coefficients above $R^2 > 0.8$.

The results on avocado attenuation (Fig. 5) decreased from day 0 to day 3 (1.2 to <0.8 dB/mm at 100 kHz), with average values falling from 0.705 to 0.472 dB/mm. By day 7, it rose slightly to 0.481 dB/mm. This correlates with ripening-induced lignification [14], which increases fiber rigidity and reduces wave attenuation. Structural changes likely drive the observed attenuation trends; future work will research additional biochemical factors affecting wave propagation.

Fig. 6 confirms stable propagation during ripening. Phase velocities ranged from 77.6–81.6 m/s (low band), 111.5–124.2 m/s (mid), and 134.4–143.7 m/s (high). This suggests that attenuation is a more sensitive indicator of tissue changes than phase velocity in the linear profile measured and in the energy regime used in the pulsed laser.

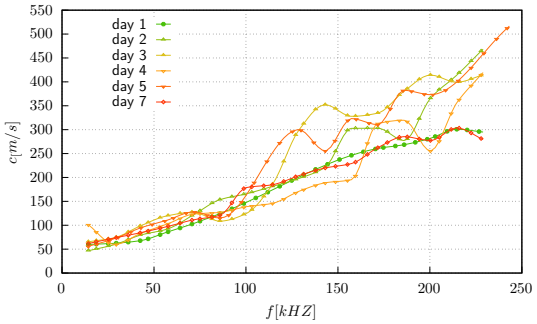

Fig. 6: Phase velocity curves for avocado samples from day 0 to day 7 of ripening.

Conclusions

The optoacoustic evaluation revealed that attenuation and phase velocity effectively reflect structural differences and ripening stages. Kiwi exhibited the highest attenuation and phase velocity, avocado showed intermediate values, and banana presented the lowest, consistent with differences in tissue hydration and stiffness. During avocado ripening, attenuation decreased markedly in early stages due to structural transformations like exocarp lignification, increasing rigidity and altering tissue contrast, thereby affecting attenuation. Phase velocity remained stable, indicating lower sensitivity to early physiological changes. These findings highlight laser ultrasound as a promising tool for potential practical applications such as automated sorting, early damage detection, storage optimization, and rapid pest infestation screening.

Acknowledgments

The authors would like to thank postdoctoral researcher Evert Duran and Professor Kasper van Wijk for their support and assistance during their doctoral internship at the University of Auckland.

References

[1] C. Scruby and L. Drain. *Laser Ultrasonics: Techniques and Applications*. First. New York: Taylor & Francis Group, 1990.

[2] S. Hitchman, K. van Wijk, and Z. Davidson. "Monitoring attenuation and the elastic properties of an apple with laser ultrasound". In: *Postharvest Biology and Technology* 121 (2016), pp. 71–77.

[3] N. Hosoya et al. "Non-destructive firmness assessment of apples using a non-contact laser excitation system based on a laser-induced plasma shock wave". In: *Postharvest Biology and Technology* 128 (2017), pp. 11–17.

[4] L. A. Cobus and K. van Wijk. "Non-contact acoustic method to measure depth-dependent elastic properties of a kiwifruit". In: *Wave Motion* 119 (2023), p. 103126.

[5] N. Arai et al. "Soft Mango Firmness Assessment Based on Rayleigh Waves Generated by a Laser-Induced Plasma Shock Wave Technique". In: *Foods* 10.2 (2021).

[6] E. L. Durán, L. Adam, and I. C. Wallis. "A robust methodology for time picking and error analysis of ultrasonic waveforms and rock densities in the laboratory". In: *Geophysics* 84.2 (2019), MR85–MR97.

[7] C. Bishop. *Pattern Recognition and Machine Learning*. Springer, Jan. 2006.

[8] H. Sakoe and S. Chiba. "Dynamic programming algorithm optimization for spoken word recognition". In: *IEEE transactions on acoustics, speech, and signal processing* 26.1 (1978), pp. 43–49.

[9] E. A. Olafsdottir, S. Erlingsson, and B. Bessason. "Tool for analysis of multichannel analysis of surface waves (MASW) field data and evaluation of shear wave velocity profiles of soils". In: *Canadian Geotechnical Journal* 55.2 (2018), pp. 217–233.

[10] E. Á. Ólafsdóttir. "Multichannel analysis of surface waves for assessing soil stiffness". MA thesis. University of Iceland, 2016.

[11] J. Taipodia, A. Dey, and D. Baglari. "Influence of data acquisition and signal preprocessing parameters on the resolution of dispersion image from active MASW survey". In: *Journal of Geophysics and Engineering* 15.4 (2018), pp. 1310–1326.

[12] B. R. Cox and D. P. Teague. "Layering ratios: a systematic approach to the inversion of surface wave data in the absence of a priori information". In: *Geophysical Journal International* 207.1 (2016), pp. 422–438.

[13] C. B. Park, R. D. Miller, and J. Xia. "Imaging dispersion curves of surface waves on multichannel record". In: *SEG technical program expanded abstracts 1998*. Society of Exploration Geophysicists, 1998, pp. 1377–1380.

[14] R. Espinosa-Velázquez et al. "Morpho-structural description of unripe and ripe avocado pericarp (Persea americana Mill var. drymifolia) descripción". In: *Revista Mexicana de Ingeniería Química* 15.2 (2016), pp. 469–480.